Biochimica et Biophysica Acta 1848 (2015) 211–219

Contents lists available at ScienceDirect

Biochimica et Biophysica Acta

journal homepage: www.elsevier.com/locate/bbamem

Review

How polyunsaturated fatty acids modify molecular organization in membranes: Insight from NMR studies of model systems☆

Saame Raza Shaikh [a], Jacob J. Kinnun [b], Xiaoling Leng [b], Justin A. Williams [b], Stephen R. Wassall [b,*]

[a] Department of Biochemistry & Molecular Biology, East Carolina Diabetes and Obesity Institute, East Carolina University, 115 Heart Drive, Room 4117, Mail Stop 743, Greenville, NC 27834, USA
[b] Department of Physics, Indiana University-Purdue University Indianapolis, 402 N. Blackford Street, Indianapolis, IN 46202-3273, USA

ARTICLE INFO

Article history:
Received 18 March 2014
Accepted 23 April 2014
Available online 9 May 2014

Keywords:
Eicosapentaenoic acid (EPA)
Docosahexaenoic acid (DHA)
Lipid microdomain
Lipid raft
Solid state ^{2}H NMR

ABSTRACT

Marine long chain n-3 polyunsaturated fatty acids (PUFA), eicosapentaenoic (EPA) and docosahexaenoic acid (DHA), are bioactive molecules with clinical applications for the treatment of several diseases. In order to effectively translate these molecules into clinical trials, it is essential to establish the underlying mechanisms for n-3 PUFA. This review focuses on efforts to understand how EPA and DHA, upon incorporation into plasma membrane phospholipids, remodel the molecular organization of cholesterol-enriched lipid microdomains. We first give an overview of results from studies on cells. Paradoxical data generated from mouse studies indicate that EPA and DHA incorporate into lipid microdomains, yet in spite of their high disorder increase molecular order within the domain. We then spotlight the utility of solid state ^{2}H NMR spectroscopy of model bilayers as a tool for elucidating underlying mechanisms by which n-3 PUFA-containing phospholipids can regulate molecular organization of lipid microdomains. Evidence is presented demonstrating that n-3 PUFA exert differential structural effects when incorporated into phosphatidylethanolamines (PE) compared to phosphatidylcholines (PC), which explains some of the conflicting results observed in vivo. Recent studies that reveal differences between the interactions of EPA and DHA with lipid microdomains, potentially reflecting a differential in bioactivity, are finally described. Overall, we highlight the notion that NMR experiments on model membranes suggest a complex model by which n-3 PUFA reorganize lipid microdomains in vivo. This article is part of a Special Issue entitled: NMR Spectroscopy for Atomistic Views of Biomembranes and Cell Surfaces. Guest Editors: Lynette Cegelski and David P. Weliky.

Contents

Abbreviations: AA, arachidonic acid; DAPC, 1,2-diarachidonylphosphatidylcholine; DHA, docosahexaenoic acid; EPA, eicosapentaenoic acid; NMR, nuclear magnetic resonance; PC, phosphatidylcholine; PE, phosphatidylethanolamine; PDPC, 1-palmitoyl-2-docosahexaenoylphosphatidylcholine; POPC, 1-palmitoyl-2-oleoylphosphatidylcholine; PUFA, polyunsaturated fatty acid; SEPC, 1-stearoyl-2-eicosapentaenoylphosphatidylcholine; SDPC, 1-stearoyl-2-docosahexaenoylphosphatidylcholine; SOPC, 1-stearoyl-2-oleoylphosphatidylcholine

☆ This article is part of a Special Issue entitled: NMR Spectroscopy for Atomistic Views of Biomembranes and Cell Surfaces. Guest Editors: Lynette Cegelski and David P. Weliky.

* Corresponding author. Tel.: +1 317 274 6908; fax: +1 317 274 2393.
E-mail address: swassall@iupui.edu (S.R. Wassall).

http://dx.doi.org/10.1016/j.bbamem.2014.04.020
0005-2736/

1. Overview

The consumption of eicosapentaenoic (EPA, 20:5) and docosahexaenoic (DHA, 22:6) acids (Fig. 1), long chain omega-3 polyunsaturated fatty acids (n-3 PUFA) found in marine oils, is low in the Western diet due to increased consumption of n-6 PUFAs [1]. Numerous clinical studies suggest potential benefits of n-3 PUFA consumption on various disease endpoints [2]. Therefore, there is tremendous interest in increasing the dietary intake for the general public and for select clinical populations through the use of n-3 PUFA enriched over-the-counter and prescription supplements. A major impediment to clinical translation is an incomplete understanding of the mechanism of action. The mechanisms for EPA and DHA are highly pleiotropic and include serving as substrates for the generation of specialized pro-resolving lipid mediators, changes in gene expression, disruption of cytoskeletal organization, modification of gene expression, serving as a ligand to GPR120 and alteration of plasma membrane microstructure [3].

This review focuses on the incorporation of n-3 PUFA into phospholipids (Fig. 2a) and their role in remodeling the architecture of plasma membrane signaling lipid microdomains. Lipid microdomains, commonly referred to as rafts, are highly ordered regions enriched in sphingolipids and cholesterol (Fig. 2b) that serve to increase the proximity of signaling proteins and thereby enhance cellular function [4]. We begin with a survey of results obtained with biological membranes followed by the insight gleaned from solid state ^{2}H NMR studies of model membranes.

2. Murine and cell culture studies

2.1. n-3 PUFA incorporate directly into crude lipid domains and displace cholesterol

Over the past decade, in vitro studies with a variety of cell types have revealed that EPA or DHA incorporate directly into membrane fractions that are detergent resistant (DRM, detergent resistant membranes) and crudely correspond to rafts [5–9]. The incorporation of n-3 PUFA into DRM is generally into the most abundant phospholipids, i.e. phosphatidylcholine (PC) and phosphatidylethanolamine (PE) [10,11]. Highly similar results were reported with in vivo studies in which the diets of rodents were supplemented with n-3 PUFA ethyl esters or marine oils [12,13]. The increase of n-3 PUFA levels in DRM is usually accompanied by a significant reduction in the n-6 PUFA arachidonic acid (AA), a highly disordered fatty acid [3,14]. As a consequence of the change in DRM fatty acid composition with n-3 PUFA, a significant change in the lateral organization of plasma membrane signaling proteins is routinely observed with cells from culture and from animals [5,7,13,15–18].

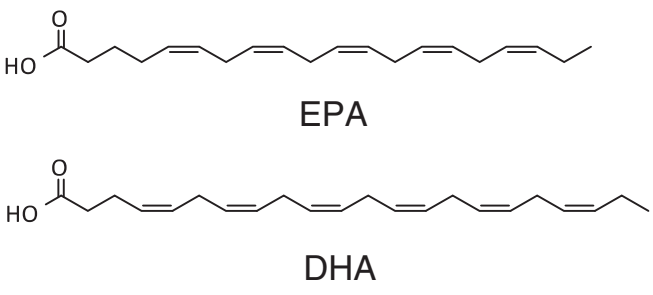

Fig. 1. Molecular structures of EPA (20:5$\Delta^{5,8,11,14,17}$) and DHA (22:6$\Delta^{4,7,10,13,16,19}$).

Several laboratories have addressed the impact of the uptake of EPA and DHA into DRM on the lateral distribution of cholesterol. The recognition that cholesterol plays a key role in the formation of ordered lipid microdomains was the motivation for the studies [4]. An increasing number of these studies have shown that n-3 PUFA lower the levels of cholesterol in DRM, which is hypothesized to be the mechanism by which protein lateral organization and subsequent signaling is modified with n-3 PUFA [19,20]. The consequence of lowering the amount of cholesterol in DRM with n-3 PUFA on the detergent soluble fraction of a membrane (DSM, detergent soluble membranes) remains unclear. There are observations that are consistent with the notion that n-3 PUFA have a poor affinity for cholesterol as revealed in studies of model membranes that will be described below [21–24]. The treatment of a neuroblast-like cell line, for example, was shown to displace cholesterol from DRM to DSM [19]. Similarly, it was recently reported that a diol of DHA relocated cholesterol from DRM to DSM in a glia cell line [25].

In some cell types such as breast cancer cells, cholesterol levels in DRM were lowered upon incorporation of n-3 PUFA into the DRM with no change in DSM cholesterol levels [6]. One explanation for the specific reduction in DRM cholesterol is that cholesterol associated with rafts is internalized into the cell in response to n-3 PUFA. Lee et al. showed that treatment of cells with DHA decreased raft-associated cholesterol levels and expression of GM1 (a marker for rafts) on the plasma membrane surface [26]. The reduction in cholesterol was driven by internalization of the lipids into lysosomes. Thus, n-3 PUFA appear in some cell types to promote internalization of lipid microdomains. An additional mechanism by which n-3 PUFA remodel DRMs may be that EPA and DHA incorporate directly into sphingolipids or esterify cholesterol. Indeed, in vivo lipidomics with B cells revealed that n-3 PUFAs incorporate directly into sphingolipids and can esterify cholesterol [11,27].

2.2. n-3 PUFA increase the molecular order of lipid microdomains

Although biochemical studies have established that n-3 PUFA incorporate into DRM and displace cholesterol, there are significant limitations to this approach. The most obvious is the use of detergent, which introduces artifacts and does not accurately model the nanoscale architecture of lipid microdomains [28]. Therefore, a few studies have attempted to understand how n-3 PUFA impact the molecular order of lipid microdomains using quantitative imaging with polarity sensitive probes. These studies revealed, contrary to expectation, that n-3 PUFA increase the molecular order of lipid microdomains.

Experiments with mouse models showed that n-3 PUFA enhance the formation of ordered lipid microdomains on the T cell side of the immunological synapse, the highly organized cholesterol-dependent interface between CD4$^+$ T cells and antigen presenting cells. The molecular order of the immunological synapse was increased by n-3 PUFA, as measured by two-photon fluorescence of the polarity sensitive probe Laurdan, accompanied by significant remodeling of the actin cytoskeleton [16,29,30]. These studies also revealed that the changes in the molecular order of the synapse with n-3 PUFA have an impact on the recruitment of select proteins into the synapse, which lead to a suppression in downstream T cell activation and proliferation [16,29].

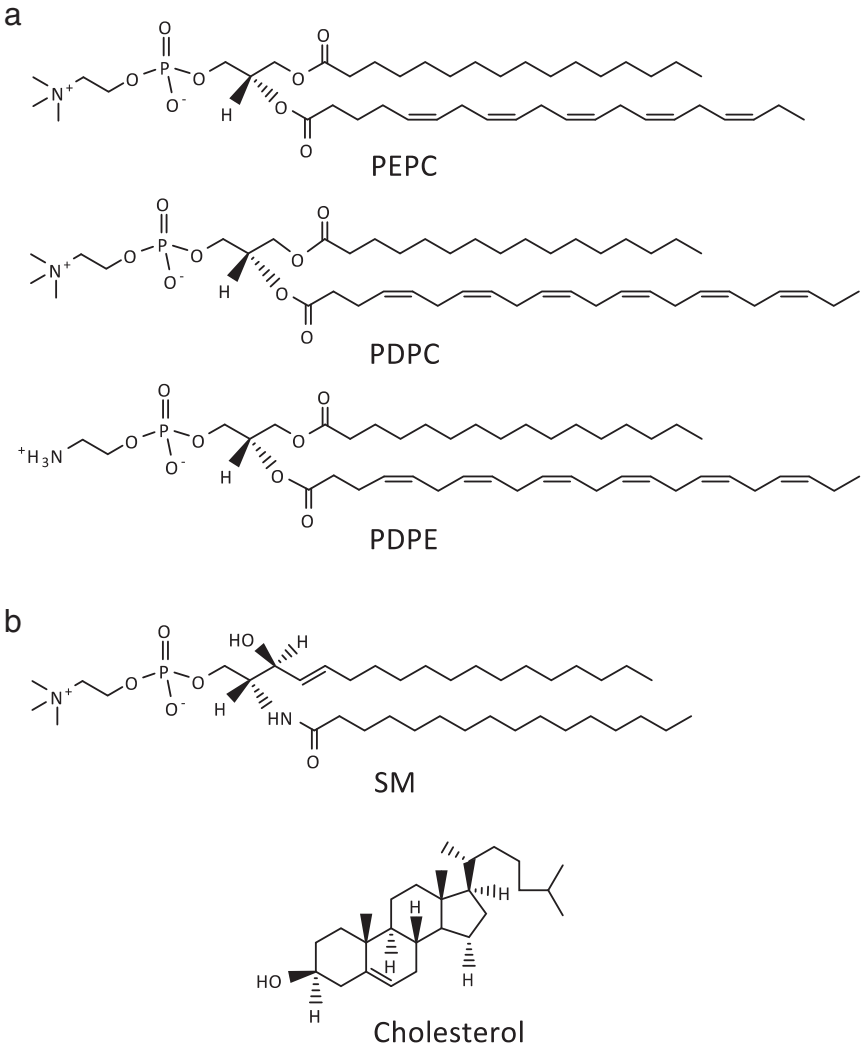

Fig. 2. Representative molecular structures of a. PUFA-containing phospholipids PEPC, PDPC and PDPE; and b. raft-forming lipids SM and cholesterol.

In another set of studies, n-3 PUFA were found to target the spatial distribution and order of lipid microdomains on the surface of B lymphocytes and EL4 T lymphomas [11]. n-3 PUFA administered to mice decreased the clustering of lipid microdomains that were induced to form in response to cholera toxin subunit b clustering of GM1 molecules. Nearly identical results were observed upon treatment of EL4 cells with DHA, but not EPA. This observation was interpreted in terms of an increase in the size of the lipid microdomains, based on confocal imaging of GM1 clusters on a micron scale. Whether n-3 PUFA actually increased the size of the clusters is debatable though, since nanoscale measurements were not conducted in parallel with appropriate high-resolution imaging.

Subsequent studies showed that B cells isolated from mice consuming n-3 PUFA displayed a reduction in generalized polarization of di-4-ANEPPDHQ, demonstrating a decrease in microviscosity with n-3 PUFA [11]. Relative to the absence of crosslinking, however, n-3 PUFA increased the polarization of di-4-ANEPPDHQ upon crosslinking GM1 molecules. Again, the change in lipid microdomain organization with n-3 PUFA disrupted the ability of a protein to accumulate on the B cell side of the immunological synapse, as demonstrated with FRET and confocal imaging, which led to suppressed cellular function [15]. The effects were recapitulated, furthermore, in the absence of n-3 PUFA with cholesterol depletion suggesting a cholesterol-mediated mechanism. The ordering effect upon lipid microdomain formation was found to be more robust with DHA than EPA in cell culture studies [11].

2.3. The paradox of biochemical and imaging studies on n-3 PUFA

A clear paradox emerges from the biochemical and imaging studies. How n-3 PUFA acyl chains, which are highly disordered structures, incorporate directly into lipid microdomains yet increase the molecular order is a mystery. Thus, the mechanism by which n-3 PUFA modifies the molecular order and formation of cholesterol-enriched microdomains remains elusive. One approach to solving this problem is to use protein-free model bilayers of controlled composition to elucidate the basic molecular interactions between n-3 PUFA-containing phospholipids, cholesterol and sphingolipids. We now direct the reader's attention to the application of solid state ^{2}H NMR spectroscopy in this endeavor. The salient features of the method and what has been learnt about the molecular organization of n-3 PUFA-containing phospholipids are first briefly covered, and then advances made in the past several years on how specific species of n-3 PUFA-containing phospholipid differentially interact with lipid microdomains are highlighted.

3. Solid state ^{2}H NMR of model membranes

Solid state ^{2}H NMR of deuterated analogs of lipid molecules offers an essentially non-invasive method for studying molecular organization within membranes. Isotopic substitution of ^{2}H for ^{1}H constitutes a minimal perturbation, while interpretation of the spectra is relatively

straightforward due to the intra-molecular nature of the quadrupolar interaction that dominates the spectral shape. There are excellent reviews, for instance by Davis [31], that give a comprehensive treatment of spectral analysis. The description here is meant merely to aid an appreciation of the data that will be discussed.

The spectrum for 1-[$^2H_{31}$]palmitoyl-2-oleoylphosphatidylcholine ([$^2H_{31}$]16:0-18:1PC, POPC-d_{31}) at 30 °C exemplifies the form of spectra obtained with analogs of phospholipids that are perdeuterated throughout a saturated *sn*-1 chain in the physiologically relevant lamellar liquid crystalline state (Fig. 3a, upper) [32]. Because the sample consists of bilayers randomly oriented in an aqueous medium relative to the direction of the magnetic field, the spectrum is a powder pattern that is comprised of a superposition of signals from bilayers at all orientations. At each orientation, moreover, the signal is a superposition of doublets from each position of deuteration along the perdeuterated *sn*-1 chain. The resultant spectrum has well defined edges at ~±13 kHz due to a plateau region of virtually constant order for methylene groups in the upper portion of the chain, while the individual peaks within the spectrum arise from less ordered methylene groups in the lower portion of the chain and the highly disordered terminal methyl group produces the central pair of peaks.

3.1. Moment analysis

Lineshape analysis is the way details of molecular organization are extracted from the spectrum [31]. The first moment

$$M_1 = \frac{\int_{-\infty}^{\infty} |\omega| f(\omega) d\omega}{\int_{-\infty}^{\infty} f(\omega) d\omega} \tag{1}$$

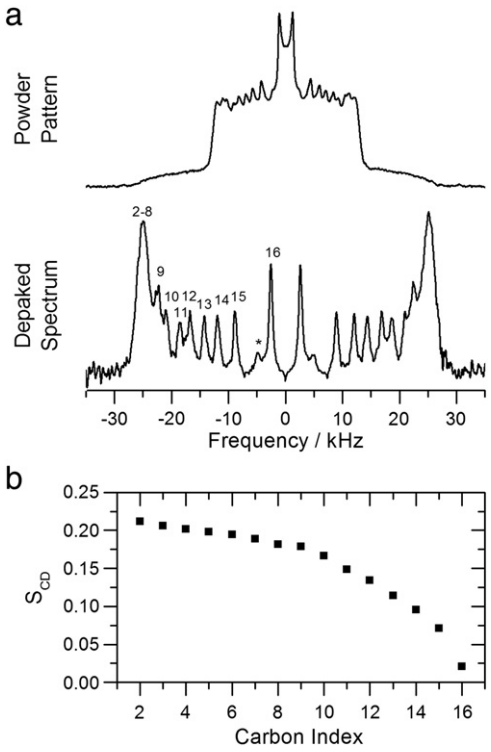

Fig. 3. ^{2}H NMR of POPC-d_{31} bilayers at 30 °C. a. Powder pattern (upper) and depaked (lower) spectra, and b. an order parameter profile derived from the depaked spectrum. The numbers next to peaks in the depaked spectrum designate the carbon positions to which they are assigned, while the asterisk is an artifact associated with the depaking algorithm that is ignored [37].

is related to the average order parameter $\bar{S}_{CD}$ for the perdeuterated *sn*-1 chain by

$$M_1 = \frac{\pi}{\sqrt{3}} \left(\frac{e^2 qQ}{h} \right) |\bar{S}_{CD}|. \tag{2}$$

In these equations ω is the frequency relative to the central Larmor frequency ω_0, $f(\omega)$ is the lineshape and $\left(\frac{e^2qQ}{h}\right) = 168$ kHz is the static quadrupolar coupling constant. The order parameter is defined according to

$$S_{CD} = \frac{1}{2} \left\langle 3\cos^2\beta - 1 \right\rangle, \tag{3}$$

where β is the time-dependent angle that the C–^{2}H bond in a methylene or methyl group makes with the bilayer normal and the angular brackets denote a time average [33]. It specifies the degree of anisotropy for the motion of chain segments relative to the bilayer normal about which lipid chains rapidly reorient with axial symmetry. Values in the range $0 \le |S_{CD}| \le \frac{1}{2}$ are typically taken, the lower limit representing effectively isotropic motion while the upper limit signifies fast axial rotation in an all-*trans* configuration. The interpretation can be complicated by geometric factors due to conformational constraints imposed, for instance, by the glycerol backbone on the beginning of the *sn*-2 chain in PC bilayers [34] and by the rigidity of a double bond on the unsaturated segment in a lipid chain [35].

3.2. Depaking

A more sophisticated level of analysis is achieved with the depaking algorithm that converts the spectrum for a multilamellar dispersion to one that corresponds to a sample of single alignment [36,37]. As demonstrated for POPC-d_{31}, the depaked spectrum consists of an outermost composite doublet produced by the plateau region of similarly ordered methylene groups in the upper portion of the chain and 6 well-resolved doublets with progressively less splitting due to the disordered methylene and terminal methyl groups in the lower portion of the chain (Fig. 3a, lower). The quadrupolar splitting $\Delta\upsilon(\theta)$ for each doublet equates to an order parameter S_{CD} via

$$\Delta\upsilon(\theta) = \frac{3}{2} \left(\frac{e^2 qQ}{h} \right) |S_{CD}| P_2(\cos\theta) \tag{4}$$

where $\theta = 0°$ is the angle that the bilayer normal makes with the magnetic field and $P_2(\cos\theta)$ is the second order Legendre polynomial. Exploiting the enhanced resolution of the depaked data, a smoothed profile of the gradient of order parameter along a chain is then generated on the basis of integrated intensity assuming monotonic variation from the top to bottom of the chain [38]. The general shape of the profile plotted for POPC-d_{31}, with its plateau of slowly varying order (S_{CD} ~ 0.20) in the upper part of the chain (positions C2-9) followed by an increasing drop-off in order toward the terminal methyl end ($S_{CD} \approx 0.02$) at the center of the bilayer (positions C10-16) (Fig. 3b), is a signature of phospholipid membranes [33]. It should be borne in mind that subtleties in the variation of order within the plateau region are not discerned by this approach. The overall shape of the gradient of molecular ordering within the bilayer is nonetheless captured.

4. Molecular organization of PUFA-containing phospholipids

4.1. PUFA-containing phospholipids are highly disordered

When EPA and DHA are taken up into phospholipids in the plasma membrane, the incorporation occurs at the *sn*-2 position while a saturated fatty acid occupies the *sn*-1 position (Fig. 2a) [39]. The n-3 PUFA-containing phospholipids produced are substantially more disordered

than their more common counterparts containing less unsaturated fatty acids such as oleic acid (OA) that with just a single double bond is most abundant. This view was substantiated by ^{2}H NMR work on 1-[$^2H_{31}$] palmitoyl-2-docosahexaenoylphosphatidylcholine ([$^2H_{31}$]16:0-22:6PC, PDPC-d_{31}), a DHA-containing analog of PC with perdeuterated palmitic acid for the *sn*-1 chain, from the Brown group [40] and on 1-[$^2H_{35}$] stearoyl-2-eicosapentaenoylphosphatidylcholine ([$^2H_{35}$]18:0-20:5PC, SEPC-d_{35}) and 1-[$^2H_{35}$]stearoyl-2-docosahexaenoylphosphatidylcholine ([$^2H_{35}$]18:0–22:6PC, SDPC-d_{35}), EPA and DHA-containing analogs of PC with perdeuterated stearic acid for the *sn*-1 chain, from the Gawrisch group [41]. The behavior is illustrated by average order parameters measured for SEPC-d_{35} $\left(\bar{S}_{CD} = 0.129\right)$ and SDPC-d_{35} $\left(\bar{S}_{CD} = 0.133\right)$ at 35 °C in our laboratory. They are reduced, EPA somewhat more than DHA, by ~10% with respect to monounsaturated 1-[$^2H_{35}$]stearoyl-2-oleoylphosphatidylcholine ([$^2H_{35}$]18:0–18:1PC, SOPC-d_{35}) $\left(\bar{S}_{CD} = 0.145\right)$ with OA for the *sn*-2 chain. While the saturated *sn*-1 chain retains the same general shape of profile for the order parameter following substitution of EPA and DHA for OA at the *sn*-2 position, the change in order is inhomogeneous along the chain (Fig. 4). There is just a slight shortening (1–2 segments) and lowering ($\Delta S_{CD} < 0.01$) of the plateau region of virtually constant order in the top half. In the bottom half where order falls more rapidly, the lowering is greater and maximized near the C14 position ($\Delta S_{CD} \sim 0.03$). An increase in area for the *sn*-1 chain that becomes larger toward the terminal methyl end, which suggests a wedge shape that is fatter at the center of the PUFA-containing bilayer, is implied [41].

The tremendously high disorder of n-3 PUFA at the *sn*-2 position is responsible for the reduction in order seen for the *sn*-1 chain relative to monounsaturated equivalents. In SDPC, which has been comprehensively examined, order parameters measured throughout most of the DHA chain are very small ($S_{CD} \sim 0.01$) [42]. They are comparable to the value for the terminal methyl in the saturated *sn*-1 chain. Only at the C2 and C3 positions where the glycerol backbone restricts the initial conformation of the *sn*-2 chain are values for the order parameter appreciably higher ($S_{CD} \sim 0.1$), albeit still much less than in the *sn*-1 chain at the corresponding positions. The presence of a repeating $=CH–CH_2–CH=$ unit that accompanies the multiple double bonds in PUFA is the origin of the high disorder. The shallow energy barrier to rotation about C – C bonds within this recurring motif produces an extremely flexible structure [43]. Based upon an analysis of ^{13}C NMR relaxation times measured in magic angle spinning (MAS) experiments on SDPC, DHA chains were calculated to isomerize with correlation times that decrease from around 80 ps for carbons near the carbonyl group to a few ps approaching the terminal methyl group [44]. The isomerization is so rapid that, except for the very top, the chain explores its entire conformational space in 50 ns. Included among the torsional states adopted, as visualized in MD simulations, are bent configurations that bring the lower portion of the chain up to the membrane surface [45].

4.2. PUFA-containing phospholipids are cholesterol-phobic

Cholesterol is found in high abundance in mammalian plasma membranes, sometimes reaching as much as 45 mol% of the total lipid [46]. It globally modulates molecular organization and its unequal affinity for different lipids promotes the formation of domains [47]. The cholesterol molecule consists of a tetracyclic ring structure with a hydroxyl group at one end and a short hydrocarbon tail at the other (Fig. 2b). In membranes the hydroxyl group usually sits just below the surface while the long molecular axis extends toward the interior, lining up approximately parallel to the lipid chains [48]. PUFA chains with their multitude of rapidly changing conformations push away the rigid steroid moiety so that PUFA-containing phospholipids have poor affinity for cholesterol [49]. An affinity for PDPC that is about 50% of POPC was determined in assays of the partitioning between large unilamellar vesicles (LUV) and cyclodextrin [50,51].

A definitive demonstration of the aversion PUFA have for cholesterol comes from the ^{2}H NMR spectrum observed for [3α-$^2H_1$]cholesterol, an analog of cholesterol selectively labeled with deuterium at the 3α position, mixed with 1,2-diarachidonylphosphatidylcholine (20:4–20:4PC, DAPC) membranes in 1:1 mol amount [24]. The spectrum is comprised of a narrow component from cholesterol within the membrane superposed upon a broad component due to solid cholesterol that is excluded from the membrane. By comparing the integrated intensity of the two spectral components, a solubility of 17 mol% was estimated. This value in DAPC with arachidonic acid that has 4 double bonds at both *sn*-1 and -2 positions contrasts with less unsaturated membranes, including mixed chain PC with a saturated *sn*-1 chain and a polyunsaturated *sn*-2 chain, that can incorporate ≥50 mol% cholesterol. It is clear that most of the sterol is driven out of the membrane when contact with PUFA chains is unavoidable in the dipolyunsaturated system, neutron scattering data revealing that sterol remaining within the DAPC bilayer is forced to the center [52,53]. Measurements of solubility also establish that the affinity of cholesterol for phosphatidylethanolamine (PE) is more sensitive than PC to the presence of DHA at the *sn*-2 position (Fig. 5) [21]. Whereas the amount of cholesterol that can be introduced into SDPC (55 ± 3 mol%) [23] is not much less than POPC (65 ± 3 mol%) [54], there is an appreciable cut in the concentration that can be accommodated in 1-palmityol-2-docosahexaenoylphosphatidylethanolamine (16:0–22:6PE, PDPE) (31 ± 3 mol%) compared to 1-palmitoyl-2-oleoylphosphatidylethanolamine (16:0–18:1PE, POPE) (51 ± 3 mol%) [21]. Tighter lipid packing that accompanies the smaller headgroup of PE offers a possible explanation. Sterol and PUFA would then be brought nearer together which is unfavorable.

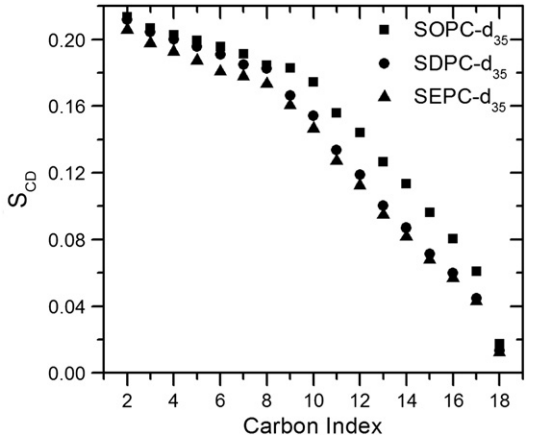

Fig. 4. Order parameter profiles derived from depaked spectra for SEPC-d_{35}, SDPC-d_{35} and SOPC-d_{35} at 35 °C.

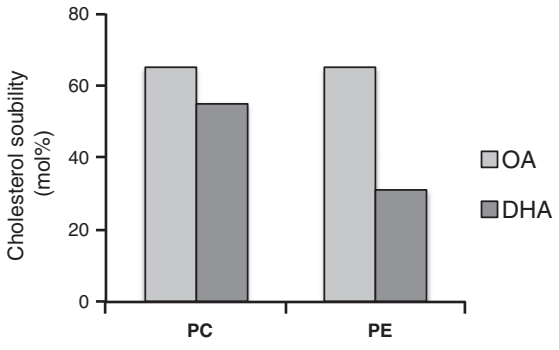

Fig. 5. Solubility of cholesterol in OA- and DHA-containing PC and PE. Values were taken from Huang et al. (POPC) [54], Brzustowicz et al. (SDPC) [24] and Shaikh et al. (POPE and PDPE) [21].

5. Molecular organization of PUFA-containing phospholipids in mixed membranes with raft-forming sphingomyelin and cholesterol

The conformational dynamics of PUFA-containing phospholipids are the complete opposite of sphingolipids found in rafts that are predominantly saturated [55]. Quadrupolar splittings recently measured for deuterated analogs of sphingomyelin (SM) (Fig. 2b), a common sphingolipid, selectively labeled in the sphingosine and amide-linked chains exhibit a profile of order resembling in form that along the *sn*-1 and -2 chains, respectively, in disaturated PC [56,57]. Ordering is particularly elevated as judged, for instance, by a comparison of an average order parameter reported for PSM-d_{31}, an analog with perdeuterated palmitic acid for the amide chain, $\left(\overline{S}_{CD} = 0.221\right)$ that is more than 50% higher than POPC-d_{31} $\left(\overline{S}_{CD} = 0.144\right)$ at the same temperature (40 °C) [58]. A preponderance of *trans* conformers within the SM chains produces a largely linear configuration that is compatible with close proximity to the smooth façade presented by the 4 rigid cycloalkane rings of cholesterol. There is consequently high affinity for the sterol [59] that is generally believed to play a fundamental role in driving the formation, as well as maintaining the stability, of lipid rafts enriched in sphingolipids and cholesterol [4].

On the one hand, the extreme disorder of n-3 PUFA-containing phospholipids suggests that their incorporation into rafts has enormous potential to modify the organized molecular architecture therein. The aversion of n-3 PUFA-containing phospholipids for cholesterol, on the other hand, suggests that they may tend to segregate into non-raft regions that are relatively poor in the sterol. Experimental evidence demonstrating that, dependent upon the species of PUFA-containing phospholipid, these two scenarios can occur in model membranes is now presented.

5.1. DHA-containing PE prefers a non-raft environment

We explored the molecular organization of PDPE in mixed membranes with SM and cholesterol in a series of publications [22,60–62]. Minimal incorporation into raft-like domains enriched in SM and cholesterol for PDPE, which instead preferentially segregates into non-raft domains that are depleted in cholesterol, was inferred from the results of a variety of techniques. ^{2}H NMR spectra recorded for PDPE-d_{31} and POPE-d_{31} (as a control), analogs with perdeuterated palmitic acid esterified at the *sn*-1 position, in mixtures with SM (1:1 mol) and with SM and cholesterol (1:1:1 mol) were important in establishing this view [22]. Representative examples acquired at 40 °C are shown in Fig. 6a. They possess the shape that is symptomatic of phospholipids in the lamellar liquid crystalline phase. Although only a single spectral component is discernible, the formation of PE-rich (less ordered) and SM-rich (more ordered) domains was concluded because the spectra differ from those for each PE individually and for PSM-d_{31} by itself or mixed with each PE [61]. The domains must be small enough to allow the deuterated analogs to exchange via lateral diffusion between them at a rate faster than the difference in the quadrupolar splitting in the two environments, and so lead to a spectrum that is a time average. An upper limit of <20 nm, corresponding to <1800 lipid molecules, was estimated taking spectra obtained for PDPE-d_{31} and PSM-d_{31} to be representative of PE-rich and SM-rich domains in PDPE/SM/cholesterol.

Close inspection of the spectra shown in Fig. 6a also reveals that broadening due to the restriction to chain motion caused by introducing cholesterol, clearly evident in the sharp shoulders associated with the plateau region of slowly varying order in the upper portion of the *sn*-1 chain, is appreciably less marked for PDPE-d_{31} (spectra on left) than POPE-d_{31} (spectra on right). As graphically depicted in Fig. 7a, the increase in average order parameter caused by the sterol that was calculated from the first moment for PDPE-d_{31} $\left(\Delta\overline{S}_{CD} = 0.039\right)$ is less than

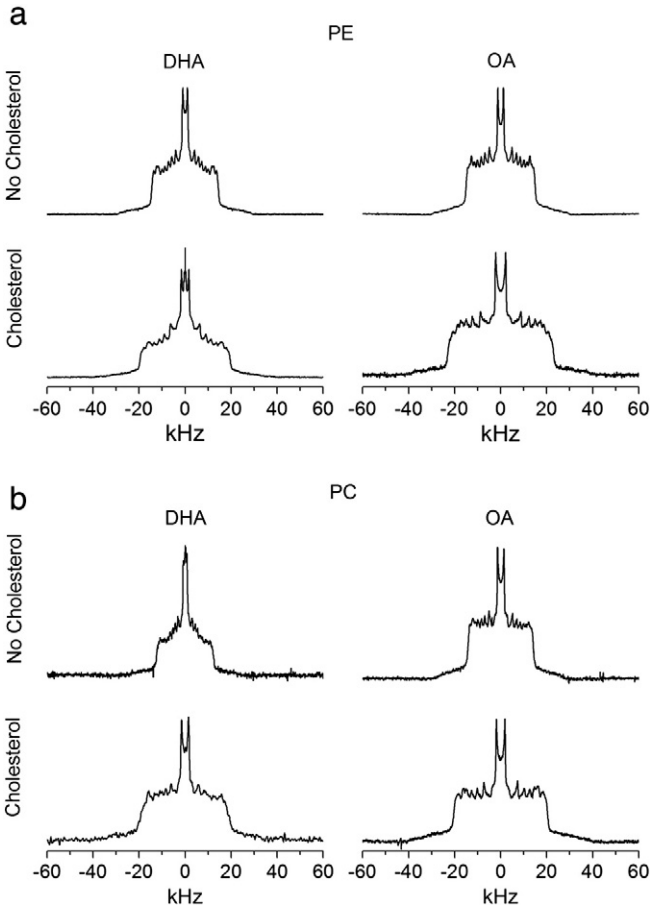

Fig. 6. ^{2}H NMR spectra at 40 °C. a. PDPE-d_{31}/SM (1:1 mol) and PDPE-d_{31}/SM/cholesterol (1:1:1 mol) (left), and POPE-d_{31}/SM (1:1 mol) and POPE-d_{31}/SM/cholesterol (1:1:1 mol) (right); and b. PDPC-d_{31}/SM (1:1 mol) and PDPC-d_{31}/SM/cholesterol (1:1:1 mol) (left), and POPC-d_{31}/SM (1:1 mol) and POPC-d_{31}/SM/cholesterol (1:1:1 mol) (right).

half for POPE-d_{31} $\left(\Delta\overline{S}_{CD} = 0.100\right)$ [22]. The smaller effect is in accord with a greater propensity to partition into domains that are sterol-poor for DHA-containing PE relative to OA-containing PE. How much PDPE-d_{31} and POPE-d_{31} distribute between domains could not be determined from the spectra. An indication comes from detergent extraction experiments conducted on PDPE/SM/cholesterol and POPE/SM/cholesterol membranes (1:1:1 mol). More than 3× as much PDPE (~70%) as POPE (~22%) was isolated in DSM ("non-raft") fractions at 4 °C, while as expected almost all SM and cholesterol (>90%) was found in DRM ("raft-like") fractions in both systems [22].

5.2. DHA-containing PC invades raft-like domains

In subsequent ^{2}H NMR studies on PDPC-d_{31} in mixed membranes with SM (1:1 mol) and with SM and cholesterol (1:1:1 mol), somewhat surprisingly in view of our results on PDPE-d_{31}, we discovered that a substantial amount of DHA-containing PC can infiltrate raft-like domains [11,63]. From an examination of the spectra plotted in Fig. 6b, it can be seen that adding cholesterol broadens the spectrum for PDPC-d_{31} (spectra on left) to a much greater extent than PDPE-d_{31} (Fig. 6a, spectra on left) at 40 °C. The increase in average order parameter due to the sterol calculated for PDPC-d_{31} $\left(\Delta\overline{S}_{CD} = 0.075\right)$ from the spectra, albeit still less than POPC-d_{31} $\left(\Delta\overline{S}_{CD} = 0.092\right)$ that constitutes our control, is nearly twice that for PDPE-d_{31} (Fig. 7b). A much greater tendency to accumulate with cholesterol and SM in domains mimicking the lipid composition of rafts is implied for PDPC over PDPE.

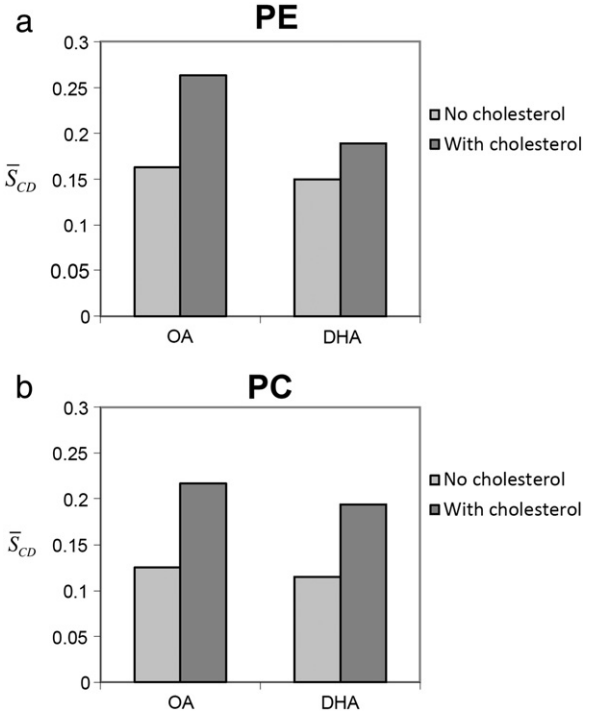

Fig. 7. Average order parameter $\overline{S}_{CD}$ derived from ^{2}H NMR spectra at 40 °C. a. PDPE-d_{31}/SM (1:1 mol) and PDPE-d_{31}/SM/cholesterol (1:1:1 mol), and POPE-d_{31}/SM (1:1 mol) and POPE-d_{31}/SM/cholesterol (1:1:1 mol); and b. PDPC-d_{31}/SM (1:1 mol) and PDPC-d_{31}/SM/cholesterol (1:1:1 mol), and POPC-d_{31}/SM (1:1 mol) and POPC-d_{31}/SM/cholesterol (1:1:1 mol).

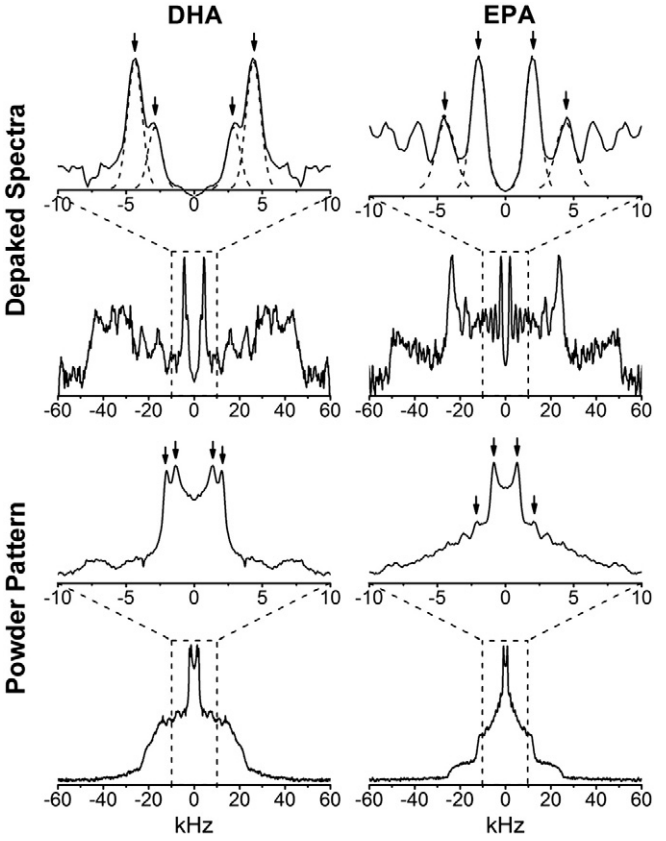

Fig. 8. ^{2}H NMR spectra at 30 °C for PDPC-d_{31}/SM/cholesterol (1:1:1 mol) (left column) and PEPC-d_{31}/SM/cholesterol (1:1:1 mol) (right column). Powder pattern (lower) and depaked (upper) spectra, together with an expansion of the central region in each case, are shown. The arrows designate pairs of signals assigned to the terminal methyl group on PDPC-d_{31} and PEPC-d_{31} in more disordered PC-rich/cholesterol-poor (inner) and more ordered SM-rich/cholesterol-rich (outer) domains. A Gaussian fit (dashed lines) was applied to the peaks in the depaked spectra.

In addition to an overall broadening, a loss of resolution within the spectrum for PDPC-d_{31}/SM is apparent following the addition of cholesterol. Individual peaks produced by methylene groups in the lower portion of the perdeuterated palmitic chain are smeared out, unlike in the spectrum for POPC-d_{31}/SM/cholesterol where the equivalent peaks remain relatively well resolved. The distinction was attributed to exchange of PDPC-d_{31} between PC-rich/cholesterol-poor and SM-rich/cholesterol-rich domains on a timescale that is comparable to, as opposed to faster than in the case of POPC-d_{31}, the difference in quadrupolar splitting for the domains [63]. A larger domain size in the DHA-containing system, on the order of the upper limit (<45 nm) estimated in the OA-containing system, was then deduced on the basis of this assessment. The transition to a spectrum at slightly lower temperature (30 °C) reflecting a slower rate exchange of exchange between domains was indicated by the splitting into two pairs of peaks (indicated by arrows in the expanded region of the spectrum) of the central signal from the terminal methyl groups in PDPC-d_{31} (Fig. 8, bottom left) [63]. With the enhanced resolution achieved by depaking, that there is much greater intensity in the outer doublet assigned to the more ordered SM-rich/cholesterol-rich domain than in inner doublet assigned to the more-disordered PC-rich/cholesterol-poor (non-raft) domain becomes clear (Fig. 8, top left). The majority of the DHA-containing PC (~70%) was found in the raft-like domain. Because PC is less averse to cholesterol than PE, we proposed PDPC is more able than PDPE to infiltrate a sterol-rich environment.

^{2}H NMR spectra collected in parallel for PEPC-d_{31}/SM/cholesterol (1:1:1 mol), on the contrary, established that the EPA-containing PC is largely confined to non-raft regions [63]. The powder pattern spectrum at 30 °C included in Fig. 8 (bottom right) is comprised of a narrow component with edges at ±12 kHz that resembles the spectrum in the absence of cholesterol superposed upon a broad component with edges at ±23 kHz. Slow exchange of PEPC-d_{31} between PC-rich/cholesterol-poor and SM-rich/cholesterol-rich domains to which, respectively, these two spectral components were ascribed that must be >35 nm in size to result in their individual observation was our interpretation [64]. From the relative intensity of the pair doublets due to the terminal methyl groups (identified by arrows) resolved in the depaked spectrum (Fig. 8, upper right), most of the PEPC-d_{31} (~60%) was identified as being in the non-raft domain. Slightly higher disorder for PEPC-d_{31} than PDPC-d_{31}, as was observed when comparing order parameter profiles for SEPC-d_{35} vs. SDPC-d_{35} (Fig. 4), may render the EPA-containing PC less compatible with insertion into an ordered domain.

6. Summary

In conclusion, a window into the complexity by which n-3 PUFA can reorganize lipid microdomains emerges from studies on lipid bilayers by solid state ^{2}H NMR spectroscopy supplemented by complementary biophysical techniques. Solid state ^{2}H NMR experiments on PDPE-d_{31}/SM/cholesterol (1:1:1 mol) showed that when DHA is esterified to PE, it segregates away from raft-like regions enriched in SM and cholesterol that are nano-scale in size. This segregation is driven by steric incompatibility between highly disordered DHA chains and the rigid steroid moiety of the sterol that is accentuated with the small head group of PE. ^{2}H NMR spectra for PDPC-d_{31}/SM/cholesterol (1:1:1 mol) indicated, contrastingly, that DHA esterified to PC infiltrates SM-rich/sterol-rich nano-sized domains. These findings provide unprecedented mechanistic insight into results from in vivo experiments on how n-3 PUFA disrupt lipid microdomains.

How the introduction of DHA-containing PE into a region of bulk lipid surrounding a raft-like domain has the potential to push cholesterol into the raft and so increase molecular order within the domain is illustrated in a cartoon presented in Fig. 9 (upper panel). This scenario, although agreeing with the increased order observed in cells treated with n-3 PUFA, does not reconcile with the redistribution of cholesterol from DRM to DSM seen in cells by detergent extraction. One intriguing possibility is to speculate that n-3 PUFA-containing PE molecules form nanodomains, which is compatible with the size indicated by NMR in model membranes, within a host microdomain that becomes more ordered because sphingolipid as well as cholesterol molecules are expelled. The NMR data establish that n-3 PUFA-containing PC can incorporate into raft-like domains in lipid bilayers, consistent with detergent extraction studies on cells that detected the uptake of EPA and DHA into DRM. What the presence of PDPC or PEPC does to molecular organization within the SM-rich/cholesterol-rich domain formed in the model membrane is yet to be studied and experiments with PSM-d_{31} are planned to directly probe order therein. It is an issue that has to be addressed since the introduction of n-3 PUFA-containing PC into an ordered raft-like domain, as depicted in a cartoon in Fig. 9 (lower panel), would be expected to displace sterol and disorder the domain. The reverse, an increase in order, is typically reported in cells. A possible explanation, interestingly, may lie in the reduction in the concentration of AA in DRM that usually follows elevation in the amount of n-3 PUFA. Order parameters measured for PDPC-d_{31} are higher (~6% in the plateau region) than 1-[$^2H_{31}$]palmitoyl-2-arachidonylphosphatidylcholine ([$^2H_{31}$]16:0–20:4PC, PAPC-d_{31}) [14], so that substituting DHA for AA could be responsible for a rise in order.

In order to develop a complete mechanism by which n-3 PUFA remodel lipid-protein signaling microdomains, extensive new studies are still needed in several areas. One, it will be necessary to develop a better understanding of how n-3 PUFA, upon uptake into other lipid species (e.g. PS), impact the molecular organization of lipid microdomains at the molecular and cellular levels. Second, the importance of structural differences between n-3 PUFA is unknown. Elucidating the effects of shorter chain n-3 PUFA such as α-linolenic acid (18:3) and stearidonic acid (18:4) is an entirely new area of investigation. In addition, it is not clear how EPA, its elongation production, DPA (22:5), and DHA differ in their ability to target lipid microdomains. Recent studies on lipid bilayers and cellular systems have shown that EPA and DHA exert different effects on lipid microdomain size and order. To develop methods that further bridge the gap between model membranes and in vivo experiments will ultimately aid our understanding of the underlying mechanisms by which n-3 PUFA remodel the architecture of cellular membranes.

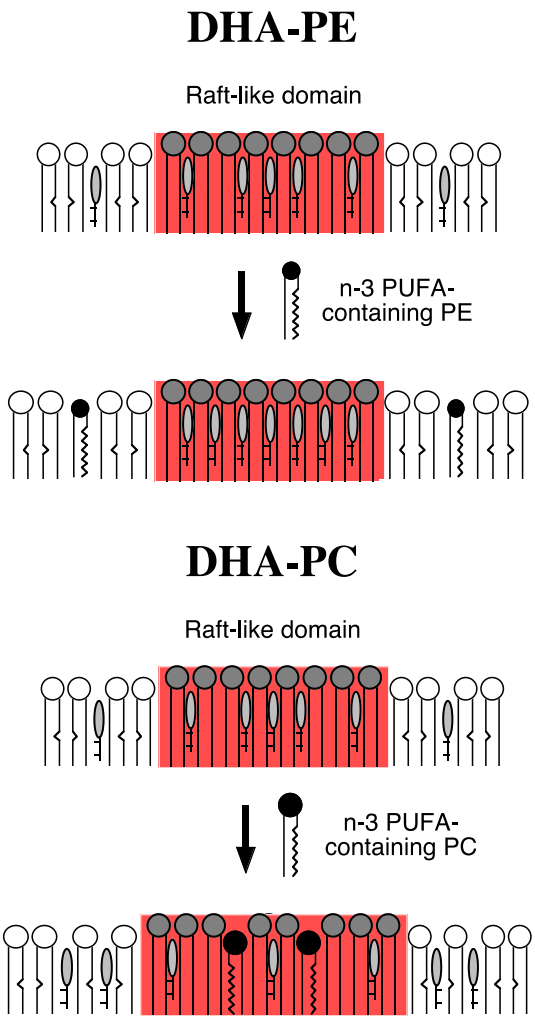

Fig. 9. Schematic representation of the incorporation of n-3 PUFA-containing phospholipids into a lipid monolayer. The monolayer is comprised of a (raft-like) domain enriched in sphingolipid and cholesterol that is flanked on each side by a (non-raft) region containing monounsaturated phospholipid (bulk lipid) and depleted in cholesterol. In the upper panel n-3 PUFA-containing PE prefers the non-raft region, redistributing cholesterol into the raft-like domain that becomes more ordered. In the lower panel n-3 PUFA-containing PC infiltrates the raft-like region, from which cholesterol is displaced into the non-raft region and which becomes more disordered.

References

[1] A.P. Simopoulos, The importance of the omega-6/omega-3 fatty acid ratio in cardiovascular disease and other chronic diseases, Exp. Biol. Med. 233 (2008) 674–688.
[2] A. Gil, L. Serra-Majem, P.C. Calder, R. Uauy, Systematic reviews of the role of omega-3 fatty acids in the prevention and treatment of disease, Br. J. Nutr. 107 (Suppl. 2) (2012) S1–S2.
[3] P.C. Calder, Mechanisms of action of (n-3) fatty acids, J. Nutr. 142 (2012) 592S–599S.
[4] D. Lingwood, K. Simons, Lipid rafts as a membrane-organizing principle, Science 327 (2010) 46–50.
[5] T.M. Stulnig, J. Huber, N. Leitinger, E.-M. Imre, P. Angelisová, P. Nowotny, W. Waldhäusl, Polyunsaturated eicosapentaenoic acid displaces proteins from membrane rafts by altering raft lipid composition, J. Biol. Chem. 276 (2001) 37335–37340.
[6] P.D. Schley, D.N. Brindley, C.J. Field, (n-3) PUFA alter raft lipid composition and decrease epidermal growth factor receptor levels in lipid rafts of human breast cancer cells, J. Nutr. 137 (2007) 548–553.
[7] S.R. Shaikh, B.D. Rockett, M. Salameh, K. Carraway, Docosahexaenoic acid modifies the clustering and size of lipid rafts and the lateral organization and surface expression of MHC class I of EL4 cells, J. Nutr. 139 (2009) 1632–1639.
[8] Q. Li, M. Wang, L. Tan, C. Wang, J. Ma, N. Li, Y. Li, G. Xu, J. Li, Docosahexaenoic acid changes lipid composition and interleukin-2 receptor signaling in membrane rafts, J. Lipid Res. 46 (2005) 1904–1913.
[9] A. Briolay, R. Jaafar, G. Nemoz, L. Bessueille, Myogenic differentiation and lipid-raft composition of L6 skeletal muscle cells are modulated by PUFAs, Biochim. Biophys. Acta 1828 (2013) 602–613.
[10] S. Zhao, L. Jia, P. Gao, Q. Li, X. Lu, J. Li, G. Xu, Study on the effect of eicosapentaenoic acid on phospholipids composition in membrane microdomains of tight junctions of epithelial cells by liquid chromatography/electrospray mass spectrometry, J. Pharm. Biomed. Anal. 47 (2008) 343–350.
[11] B.D. Rockett, H. Teague, M. Harris, M. Melton, J. Williams, S.R. Wassall, S.R. Shaikh, Fish oil increases raft size and membrane order of B cells accompanied by differential effects on function, J. Lipid Res. 53 (2012) 674–685.
[12] Y.-Y. Fan, D.N. McMurray, L.H. Ly, R.S. Chapkin, Dietary (n-3) polyunsaturated fatty acids remodel mouse T-cell lipid rafts, J. Nutr. 133 (2003) 1913–1920.
[13] Y.Y. Fan, L.H. Ly, R. Barhoumi, D.N. McMurray, R.S. Chapkin, Dietary docosahexaenoic acid suppresses T cell protein kinase C theta lipid raft recruitment and IL-2 production, J. Immunol. 173 (2004) 6151–6160.
[14] K. Rajamoorthi, H.I. Petrache, T.J. McIntosh, M.F. Brown, Packing and viscoelasticity of polyunsaturated ω-3 and ω-6 lipid bilayers as seen by ^2H NMR and X-ray diffraction, J. Am. Chem. Soc. 127 (2005) 1576–1588.
[15] B.D. Rockett, M. Melton, M. Harris, L.C. Bridges, S.R. Shaikh, Fish oil disrupts MHC class II lateral organization on the B-cell side of the immunological synapse independent of B-T cell adhesion, J. Nutr. Biochem. 24 (2013) 1810–1816.
[16] W. Kim, Y.Y. Fan, R. Barhoumi, R. Smith, D.N. McMurray, R.S. Chapkin, n-3 Polyunsaturated fatty acids suppress the localization and activation of signaling proteins at the immunological synapse in murine CD4 + T cells by affecting lipid raft formation, J. Immunol. 181 (2008) 6236–6243.
[17] F. Aliche-Djoudi, N. Podechard, A. Collin, M. Chevanne, E. Provost, M. Poul, L. Le Hégarat, D. Catheline, P. Legrand, M.-T. Dimanche-Boitrel, D. Lagadic-Gossmann, O. Sergent, A role for lipid rafts in the protection afforded by docosahexaenoic acid against ethanol toxicity in primary rat hepatocytes, Food Chem. Toxicol. 60 (2013) 286–296.

[18] S.W. Wong, M.-J. Kwon, A.M.K. Choi, H.-P. Kim, K. Nakahira, D.H. Hwang, Fatty acids modulate toll-like receptor 4 activation through regulation of receptor dimerization and recruitment into lipid rafts in a reactive oxygen species-dependent manner, J. Biol. Chem. 284 (2009) 27384–27392.
[19] M.O.W. Grimm, J. Kuchenbecker, S. Grösgen, V.K. Burg, B. Hundsdörfer, T.L. Rothhaar, P. Friess, M.C. de Wilde, L.M. Broersen, B. Penke, M. Péter, L. Vígh, H.S. Grimm, T. Hartmann, Docosahexaenoic acid reduces amyloid β production via multiple pleiotropic mechanisms, J. Biol. Chem. 286 (2011) 14028–14039.
[20] S.R. Shaikh, Biophysical and biochemical mechanisms by which dietary N-3 polyunsaturated fatty acids from fish oil disrupt membrane lipid rafts, J. Nutr. Biochem. 23 (2012) 101–105.
[21] S.R. Shaikh, V. Cherezov, M. Caffrey, S.P. Soni, D. LoCascio, W. Stillwell, S.R. Wassall, Molecular organization of cholesterol in unsaturated phosphatidylethanolamines: X-ray diffraction and solid state ^{2}H NMR reveal differences with phosphatidylcholines, J. Am. Chem. Soc. 128 (2006) 5375–5383.
[22] S.R. Shaikh, A.C. Dumaual, A. Castillo, D. LoCascio, R.A. Siddiqui, W. Stillwell, S.R. Wassall, Oleic and docosahexaenoic acid differentially phase separate from lipid raft molecules: a comparative NMR, DSC, AFM, and detergent extraction study, Biophys. J. 87 (2004) 1752–1766.
[23] M.R. Brzustowicz, V. Cherezov, M. Zerouga, M. Caffrey, W. Stillwell, S.R. Wassall, Controlling membrane cholesterol content. A role for polyunsaturated (docosahexaenoate) phospholipids, Biochemistry 41 (2002) 12509–12519.
[24] M.R. Brzustowicz, V. Cherezov, M. Caffrey, W. Stillwell, S.R. Wassall, Molecular organization of cholesterol in polyunsaturated membranes: microdomain formation, Biophys. J. 82 (2002) 285–298.
[25] J. Hu, R. Popp, T. Frömel, M. Ehling, K. Awwad, R.H. Adams, H.-P. Hammes, I. Fleming, Müller glia cells regulate Notch signaling and retinal angiogenesis via the generation of 19,20-dihydroxydocosapentaenoic acid, J. Exp. Med. 211 (2014) 281–295.
[26] E.J. Lee, U.-J. Yun, K.H. Koo, J.Y. Sung, J. Shim, S.-K. Ye, K.-M. Hong, Y.-N. Kim, Down-regulation of lipid raft-associated onco-proteins via cholesterol-dependent lipid raft internalization in docosahexaenoic acid-induced apoptosis, Biochim. Biophys. Acta 1841 (2014) 190–203.
[27] H. Teague, C.J. Fhaner, M. Harris, D.M. Duriancik, G.E. Reid, S.R. Shaikh, n-3 PUFAs enhance the frequency of murine B-cell subsets and restore the impairment of antibody production to a T-independent antigen in obesity, J. Lipid Res. 54 (2013) 3130–3138.
[28] H. Heerklotz, Triton promotes domain formation in lipid raft mixtures, Biophys. J. 83 (2002) 2693–2701.
[29] W. Kim, R. Barhoumi, D.N. McMurray, R.S. Chapkin, Dietary fish oil and DHA down-regulate antigen-activated CD4+ T-cells while promoting the formation of liquid-ordered mesodomains, Br. J. Nutr. (2013) 1–7.
[30] T.Y. Hou, J.M. Monk, Y.Y. Fan, R. Barhoumi, Y.Q. Chen, G.M. Rivera, D.N. McMurray, R.S. Chapkin, n-3 Polyunsaturated fatty acids suppress phosphatidylinositol 4,5-bisphosphate-dependent actin remodelling during CD4+ T-cell activation, Biochem. J. 443 (2012) 27–37.
[31] J.H. Davis, The description of membrane lipid conformation, order and dynamics by ^{2}H-NMR, Biochim. Biophys. Acta 737 (1983) 117–171.
[32] S.R. Wassall, M.A. McCabe, C.D. Wassall, R.O. Adlof, S.E. Feller, Solid-state ^{2}H NMR and MD simulations of positional isomers of a monounsaturated phospholipid membrane: Structural implications of double bond location, J. Phys. Chem. B 114 (2010) 11474–11483.
[33] J. Seelig, Deuterium magnetic resonance theory and application to lipid membranes, Q. Rev. Biophys. 10 (1977) 353–418.
[34] A.K. Engel, D. Cowburn, The origin of multiple quadrupole couplings in the deuterium NMR spectra of the 2 chain of 1,2 dipalmitoyl-sn-glycero-3-phosphorylcholine, FEBS Lett. 126 (1981) 169–171.
[35] J. Seelig, N. Waespe-Sarcevic, Molecular order in cis and trans unsaturated phospholipid bilayers, Biochemistry 17 (1978) 3310–3315.
[36] M. Bloom, E. Sternin, A.L. MacKay, De-Pake-ing of NMR spectra, J. Magn. Reson. 55 (1983) 274–282.
[37] M.A. McCabe, S.R. Wassall, Rapid deconvolution of NMR powder spectra by weighted fast Fourier transformation, Solid State Nucl. Magn. Reson. 10 (1997) 53–61.
[38] M. Lafleur, B. Fine, E. Sternin, P.R. Cullis, M. Bloom, Smoothed orientational order profile of lipid bilayers by ^{2}H-nuclear magnetic resonance, Biophys. J. 56 (1989) 1037–1041.
[39] W. Stillwell, S.R. Wassall, Docosahexaenoic acid: membrane properties of a unique fatty acid, Chem. Phys. Lipids 126 (2003) 1–27.
[40] A. Salmon, S.W. Dodd, G.D. Williams, J.M. Beach, M.F. Brown, Configurational statistics of acyl chains in polyunsaturated lipid bilayers from deuterium NMR, J. Am. Chem. Soc. 109 (1987) 2600–2609.
[41] L.L. Holte, S.A. Peter, T.M. Sinnwell, K. Gawrisch, ^{2}H nuclear magnetic resonance order parameter profiles suggest a change of molecular shape for phosphatidylcholines containing a polyunsaturated acyl chain, Biophys. J. 68 (1995) 2396–2403.
[42] K. Gawrisch, O. Soubias, Structure and dynamics of polyunsaturated hydrocarbon chains in lipid bilayers-significance for GPCR function, Chem. Phys. Lipids 153 (2008) 64–75.
[43] S.E. Feller, Acyl chain conformations in phospholipid bilayers: a comparative study of docosahexaenoic acid and saturated fatty acids, Chem. Phys. Lipids 153 (2008) 76–80.
[44] O. Soubias, K. Gawrisch, Docosahexaenoyl chains isomerize on the sub-nanosecond time scale, J. Am. Chem. Soc. 129 (2007) 6678–6679.
[45] S.E. Feller, K. Gawrisch, A.D. MacKerell, Polyunsaturated fatty acids in lipid bilayers: intrinsic and environmental contributions to their unique physical properties, J. Am. Chem. Soc. 124 (2001) 318–326.
[46] P. Yeagle, The Membranes of Cells, 2nd ed., 1993.
[47] J.R. Silvius, Role of cholesterol in lipid raft formation: lessons from lipid model systems, Biochim. Biophys. Acta 1610 (2003) 174–183.
[48] G. Khelashvili, D. Harries, How sterol tilt regulates properties and organization of lipid membranes and membrane insertions, Chem. Phys. Lipids 169 (2013) 113–123.
[49] S.R. Wassall, W. Stillwell, Polyunsaturated fatty acid-cholesterol interactions: domain formation in membranes, Biochim. Biophys. Acta 1788 (2009) 24–32.
[50] S.-L. Niu, B.J. Litman, Determination of membrane cholesterol partition coefficient using a lipid vesicle-cyclodextrin binary system: effect of phospholipid acyl chain unsaturation and headgroup composition, Biophys. J. 83 (2002) 3408–3415.
[51] J.A. Williams, C.D. Wassall, M.D. Kemple, S.R. Wassall, An electron paramagnetic resonance method for measuring the affinity of a spin-labeled analog of cholesterol for phospholipids, J. Membr. Biol. 246 (2013) 689–696.
[52] T.A. Harroun, J. Katsaras, S.R. Wassall, Cholesterol hydroxyl group is found to reside in the center of a polyunsaturated lipid membrane, Biochemistry 45 (2006) 1227–1233.
[53] T.A. Harroun, J. Katsaras, S.R. Wassall, Cholesterol is found to reside in the center of a polyunsaturated lipid membrane, Biochemistry 47 (2008) 7090–7096.
[54] J. Huang, J.T. Buboltz, G.W. Feigenson, Maximum solubility of cholesterol in phosphatidylcholine and phosphatidylethanolamine bilayers, Biochim. Biophys. Acta 1417 (1999) 89–100.
[55] S.R. Wassall, W. Stillwell, Docosahexaenoic acid domains: the ultimate non-raft membrane domain, Chem. Phys. Lipids 153 (2008) 57–63.
[56] T. Yasuda, M. Kinoshita, M. Murata, N. Matsumori, Detailed comparison of deuterium quadrupole profiles between sphingomyelin and phosphatidylcholine bilayers, Biophys. J. 106 (2014) 631–638.
[57] N. Matsumori, T. Yasuda, H. Okazaki, T. Suzuki, T. Yamaguchi, H. Tsuchikawa, M. Doi, T. Oishi, M. Murata, Comprehensive molecular motion capture for sphingomyelin by site-specific deuterium labeling, Biochemistry 51 (2012) 8363–8370.
[58] A. Bunge, P. Müller, M. Stöckl, A. Herrmann, D. Huster, Characterization of the ternary mixture of sphingomyelin, POPC, and cholesterol: support for an inhomogeneous lipid distribution at high temperatures, Biophys. J. 94 (2008) 2680–2690.
[59] A. Tsamaloukas, H. Szadkowska, H. Heerklotz, Thermodynamic comparison of the interactions of cholesterol with unsaturated phospholipid and sphingomyelins, Biophys. J. 90 (2006) 4479–4487.
[60] S.R. Shaikh, V. Cherezov, M. Caffrey, W. Stillwell, S.R. Wassall, Interaction of cholesterol with a docosahexaenoic acid-containing phosphatidylethanolamine: trigger for microdomain/raft formation? Biochemistry 42 (2003) 12028–12037.
[61] S.P. Soni, D.S. LoCascio, Y. Liu, J.A. Williams, R. Bittman, W. Stillwell, S.R. Wassall, Docosahexaenoic acid enhances segregation of lipids between: ^{2}H-NMR study, Biophys. J. 95 (2008) 203–214.
[62] S.R. Shaikh, D.S. Locascio, S.P. Soni, S.R. Wassall, W. Stillwell, Oleic- and docosahexaenoic acid-containing phosphatidylethanolamines differentially phase separate from sphingomyelin, Biochim. Biophys. Acta 1788 (2009) 2421–2426.
[63] J.A. Williams, S.E. Batten, M. Harris, B.D. Rockett, S.R. Shaikh, W. Stillwell, S.R. Wassall, Docosahexaenoic and eicosapentaenoic acids segregate differently between raft and nonraft domains, Biophys. J. 103 (2012) 228–237.